Geophys. J. Int. (1993) **115**, 313–318

RESEARCH NOTE

On the use of the checker-board test to assess the resolution of tomographic inversions

Jean-Jacques Lévêque, Luis Rivera and Gérard Wittlinger
Institut de Physique du Globe, 5 rue René Descartes, F-67084 Strasbourg, France

Accepted 1993 February 19. Received 1993 February 18; in original form 1992 June 29

SUMMARY

This note is devoted to the confrontation of intuitive ideas in the field of inverse problems, especially in tomographic seismological studies, with the results of a more rigorous approach. With the help of a simple example, we show that tests commonly used to illustrate the quality of inversion results can be misleading. Based on a classical mathematical analysis, we explain the origin of the problems that we have seen. Our main conclusion is that, in circumstances not so unrealistic, and in contradiction to a generally accepted idea, small-size structures like in the 'checker-board test' can be well retrieved while larger structures are poorly retrieved.

Key words: inverse problems, resolution, tomography.

INTRODUCTION

In the last few years, tomographic inversion methods have become increasingly popular to provide images of the internal structure of the Earth at different scales (e.g. Dziewonski & Woodhouse 1987; Spakman 1988; Montagner & Tanimoto 1991; Evans & Achauer 1993). A difficulty commonly encountered in such methods is the estimation of the reliability of the images obtained in this way, or, in other words, knowing how close the image is to the actual structure. Modern inversion methods provide tools to do this, namely, the *a posteriori* errors and the resolution matrix (Franklin 1970). However, many authors have found these tools difficult to apply, or too expensive, and they have used a different approach based on the inversion of synthetic data. In this approach, the 'quality' criterion is the similarity between the final model and the arbitrary model used to compute the synthetics.

The aim of this note is to show that severe misinterpretations can occur using this last approach, and that the source of the problem is in the arbitrary choice of the model used to compute the synthetics.

AN ILLUSTRATIVE EXAMPLE

The example we present here as an illustration is a block inversion of amplitude data measured in a 2-D structure in order to obtain a model of the variation of attenuation in that structure.

We assume a uniform velocity in the whole medium, so that the source-to-receiver paths are straight lines. The geometry of sources and receivers and the block sampling is shown in Fig. 1.

The first arbitrary model we use is a regular pattern of high and low attenuation zones sized to the elementary block size (Fig. 2a), commonly known as the 'checker-board test'. Synthetic data are then computed and inverted using the Lanczos's (1961) method. The inverted model (Fig. 2b) is perfectly identical to the 'true' model.

The second model is a single large high attenuation block surrounded by a uniform low attenuation zone (Fig. 3a). The corresponding inverted model (Fig. 3b) shows a clear difference to the 'true' model, namely, an overestimation of the contrast between the two blocks in the left column and an underestimation of the contrast between the two blocks in the right column.

These two results are in contradictions to the generally accepted idea (e.g. Fukao *et al.* 1992) that if an inversion scheme can accurately retrieve small-size structures, it is able *a fortiori* to retrieve larger structures.

ANALYSIS OF THE PROBLEM

In order to understand what happens in the example presented above, we make a very simple mathematical description of the problem, independent of the inverse method used to solve it.

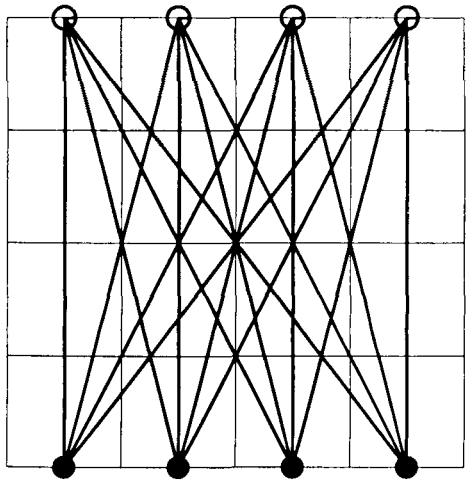

Figure 1. Geometry of the experiment: the square area is divided into 16 small blocks in which we want to know the attenuation values. Waves are emitted at four sources located at the base of the area under study, and amplitude measurements are made using the four sensors at the top of the area.

We can state the linear direct problem as:

$$\mathbf{d} = \mathbf{G} \cdot \mathbf{m}, \tag{1}$$

where $\mathbf{d}$ is the data vector, $\mathbf{m}$ is the model vector, and $\mathbf{G}$ is the linear operator which represents the theory of the experiment.

In a synthetic experiment, we compute the data vector $\mathbf{d}_s$ corresponding to the arbitrary chosen model $\mathbf{m}_s$:

$$\mathbf{d}_s = \mathbf{G} \cdot \mathbf{m}_s. \tag{2}$$

We then compute the estimated model by applying an inversion operator $\mathbf{L}$ to the synthetic data:

$$\hat{\mathbf{m}} = \mathbf{L} \cdot \mathbf{d}_s, \tag{3}$$

which can be rewritten as:

$$\hat{\mathbf{m}} = \mathbf{L} \cdot \mathbf{G} \cdot \mathbf{m}_s = \mathbf{R} \cdot \mathbf{m}_s, \tag{4}$$

where $\mathbf{R}$ is the resolution operator.

Now, to understand the paradox described above, we have to consider the following question: what is the condition to obtain an estimated model $\hat{\mathbf{m}}$ equal to the initial model $\mathbf{m}_s$?

The answer is straightforward:

$$\hat{\mathbf{m}} = \mathbf{m}_s \Leftrightarrow \mathbf{m}_s = \mathbf{R} \cdot \mathbf{m}_s, \tag{5}$$

and this last equation implies that $\mathbf{m}_s$ is an eigenvector of the resolution operator $\mathbf{R}$, associated with eigenvalue 1. This also means that the key point is the knowledge of $\mathbf{R}$.

In the example presented above, we used the linear inversion model of Lanczos (1961) which takes advantage of the singular value decomposition of $\mathbf{G}$ to build the pseudo-inverse of Moore (1920) and Penrose (1955). The corresponding resolution operator has 12 eigenvalues equal to 1 and four eigenvalues equal to 0. In that case where the eigensubspaces are multidimensional, we have to choose a

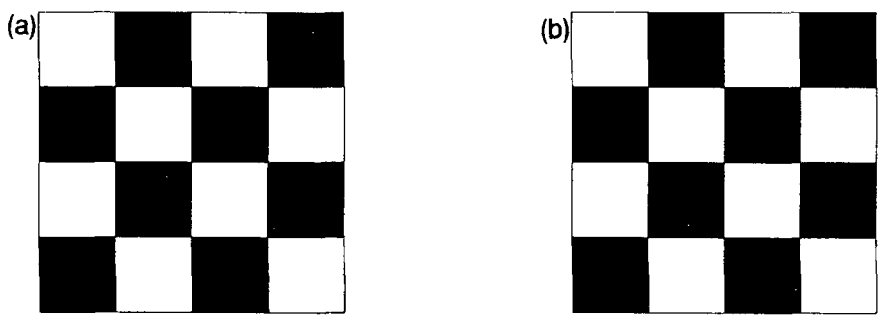

Figure 2. (a) First arbitrary model used for the computation of synthetic data: a pattern of alternate high and low attenuation elementary squares. This is the pattern used in the so-called 'checker-board test'. (b) Inverted model obtained from the synthetic data corresponding to the model in (a). It is identical with the initial model.

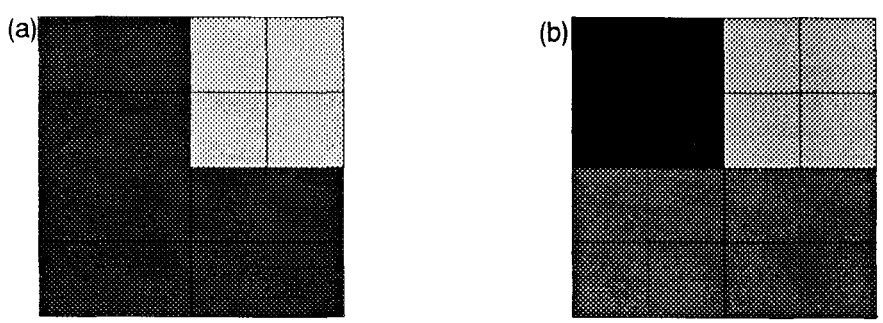

Figure 3. (a) Second arbitrary model used for the computation of synthetic data: a large zone (2×2 elementary blocks) with high attenuation (light grey) surrounded by a lower attenuation region (dark grey). (b) Inverted model obtained from the synthetic data corresponding to the model in 3(a). It differs from the initial model, showing that, for the same experimental geometry, large structures are not necessarily better retrieved than small structures (compare with Fig. 2). The grey scale is common to Figs 2, 3 and 6: lowest and highest attenuations are black and white, respectively.

basis among the number of possible bases. In Fig. 4 we present such a basis, the most natural one in our opinion, made from the eigenvectors of $\mathbf{G}^t \cdot \mathbf{G}$ which, for the Lanczos's inversion operator, are also eigenvectors of $\mathbf{R}$. We decomposed the two initial models of our experiment on this eigenbasis of $\mathbf{R}$. The reason for the paradox becomes apparent: the checker-board model has no component in the subspace of $\mathbf{R}$ associated with the eigenvalues different from 1 (Fig. 5a), while the second model, a single large block, presents a significant component in the null space of $\mathbf{R}$ (Fig. 5b).

In this example, the inverted model is the projection of the initial (arbitrary) model on to the subspace spanned by the eigenvectors related to the eigenvalue equal to 1. In the first case, the projection is equal to the initial model while in the second case, the projection leads to a real amputation of the initial model. This point can be made even more apparent by building a model only from null space eigenvectors (zero eigenvalue). Such a model is presented in Fig. 6(a) together with the corresponding inverted model (Fig. 6b). In this case, the two large blocks present in the initial model are completely missed in the inversion, and the final model is a perfectly uniform pattern. This last example clearly demonstrates the failure of the intuitive link between the characteristic wavelength of the model heterogeneities and their retrievability by a given inversion, namely, that large blocks are easier to retrieve than small blocks. When comparing Figs 2, 3 and 6, one could conclude that the larger the blocks are, the worse they are retrieved.

We would like to emphasize at this stage of the analysis that, whatever the inversion operator $\mathbf{L}$ is, the null space of $\mathbf{R}$ contains at least the null space of $\mathbf{G}$. Indeed, if one has a model $\mathbf{m}$ such that $\mathbf{G} \cdot \mathbf{m} = 0$, then $\mathbf{R} \cdot \mathbf{m} = \mathbf{L} \cdot \mathbf{G} \cdot \mathbf{m} = 0$ as well. Any strategy employed to enhance the behaviour of the inversion operator $\mathbf{L}$ will never be able to change this fact. On the other hand, if the null space of $\mathbf{G}$ is restricted to $\{0\}$, then a natural inverse of $\mathbf{G}$ exists, either $\mathbf{G}^{-1}$ if $\mathbf{G}$ is represented by a square matrix or $(\mathbf{G}^t \cdot \mathbf{G})^{-1} \cdot \mathbf{G}^t$ if $\mathbf{G}$ is a rectangular matrix. In both cases, the associated resolution would be the identity operator. There is, therefore, no need to use another inversion operator, except if some noise is added to the data. This situation will be briefly presented at the end of the paper.

Let us also remark that the problem discussed in this note is not, strictly speaking, a resolution problem, even if it is related to this concept. The resolution matrix is indeed exactly the same in the three examples we have presented since the geometry is the same in all cases and only the values of synthetic data are changed. This resolution, which acts as the same filter on the three models, simply traps nothing in the first example while it traps a significant part of the model in the second example and the whole model in the last example.

DISCUSSION

In the example described above, the resolution operator has quite a simple structure, with only two different eigenvalues, 1 and 0, and two associated subspaces of dimension 12 and four, respectively.

For other inverse operators, the situation could be slightly more complicated: there would be at least as many zero eigenvalues for $\mathbf{R}$ as for $\mathbf{G}$, due to the inclusion of the null spaces explained above, but the non-zero eigenvalues could depart from 1. We detail hereafter some remarks about the basic cases to consider when defining the initial model. If the $\lambda = 1$ eigenvalue exists, we can choose $\mathbf{m}_s$ equal to an eigenvector associated with this eigenvalue. In this case, as for the checker-board model of our experiment, we find:

$$\hat{\mathbf{m}} = \mathbf{R} \cdot \mathbf{m}_s = 1 \cdot \mathbf{m}_s = \mathbf{m}_s, \tag{6}$$

and we perfectly retrieve the initial model.

If we choose $\mathbf{m}_s$ equal to an eigenvector associated with a $\lambda \neq 0,1$ eigenvalue, we find:

$$\hat{\mathbf{m}} = \mathbf{R} \cdot \mathbf{m}_s = \lambda \cdot \mathbf{m}_s, \tag{7}$$

meaning that we perfectly retrieve the shape of the initial model, but there is a global scaling factor equal to the eigenvalue λ.

If we choose $\mathbf{m}_s$ equal to an eigenvector associated with the $\lambda = 0$ eigenvalue, we find:

$$\hat{\mathbf{m}} = \mathbf{R} \cdot \mathbf{m}_s = 0 \cdot \mathbf{m}_s. \tag{8}$$

An illustration of this situation has been presented already in Figs 6(a) and (b), where the final model is a flat zero.

If we then choose a model $\mathbf{m}_s$ which has no component in the null space of $\mathbf{R}$, but has components on subspaces associated with different non-zero eigenvalues, we find:

$$\hat{\mathbf{m}} = \mathbf{R} \cdot \mathbf{m}_s = \sum \lambda_i p_i \quad \mathbf{m}_i, \tag{9}$$

where λ_i is a non-zero eigenvalue, $\mathbf{m}_i$ is the associated eigenvector and p_i is the projection of $\mathbf{m}_s$ on that component $\mathbf{m}_i$. Model $\hat{\mathbf{m}}$ is to be compared with $\mathbf{m}_s = \sum p_i \mathbf{m}_i$. Since the λ_i are different from 1, there is a difference between $\hat{\mathbf{m}}$ and $\mathbf{m}_s$ which depends on how much $\lambda_i p_i$ differs from p_i. Note, however, that most inversion operators are (at least partially) subject to a condition of minimization of $\mathbf{R} - \mathbf{I}$, leading to non-zero eigenvalues of $\mathbf{R}$ as close to 1 as possible.

A model general enough to really provide information about the resolution would have components in every eigen-subspace. We then have a situation similar to the previous case, but with the addition of a component in the null space which is filtered out in the inverted model, thus increasing the difference between the initial and final models.

An alternative approach for assessing the resolution of the inversion would be to show several models that are perfectly retrievable, and several other models which are perfectly unretrievable. But even such a detailed presentation is still incomplete and could lead to the wrong conclusions.

Let us note that building such models requires the knowledge of the eigenvectors of $\mathbf{R}$. They can be computed by standard singular value decomposition algorithms, provided computing facilities compatible with the model space dimension are available. However the very first condition is to know explicitly this resolution operator, namely the matrix representing it. Fortunately, even for iterative linear inversion algorithms, it is possible to compute this matrix. Indeed, the ith column of $\mathbf{R}$ can be obtained by applying the inversion algorithm to the ith column of $\mathbf{G}$ (Trampert & Lévêque 1990). The knowledge of $\mathbf{R}$ is thus only a matter of computer time.

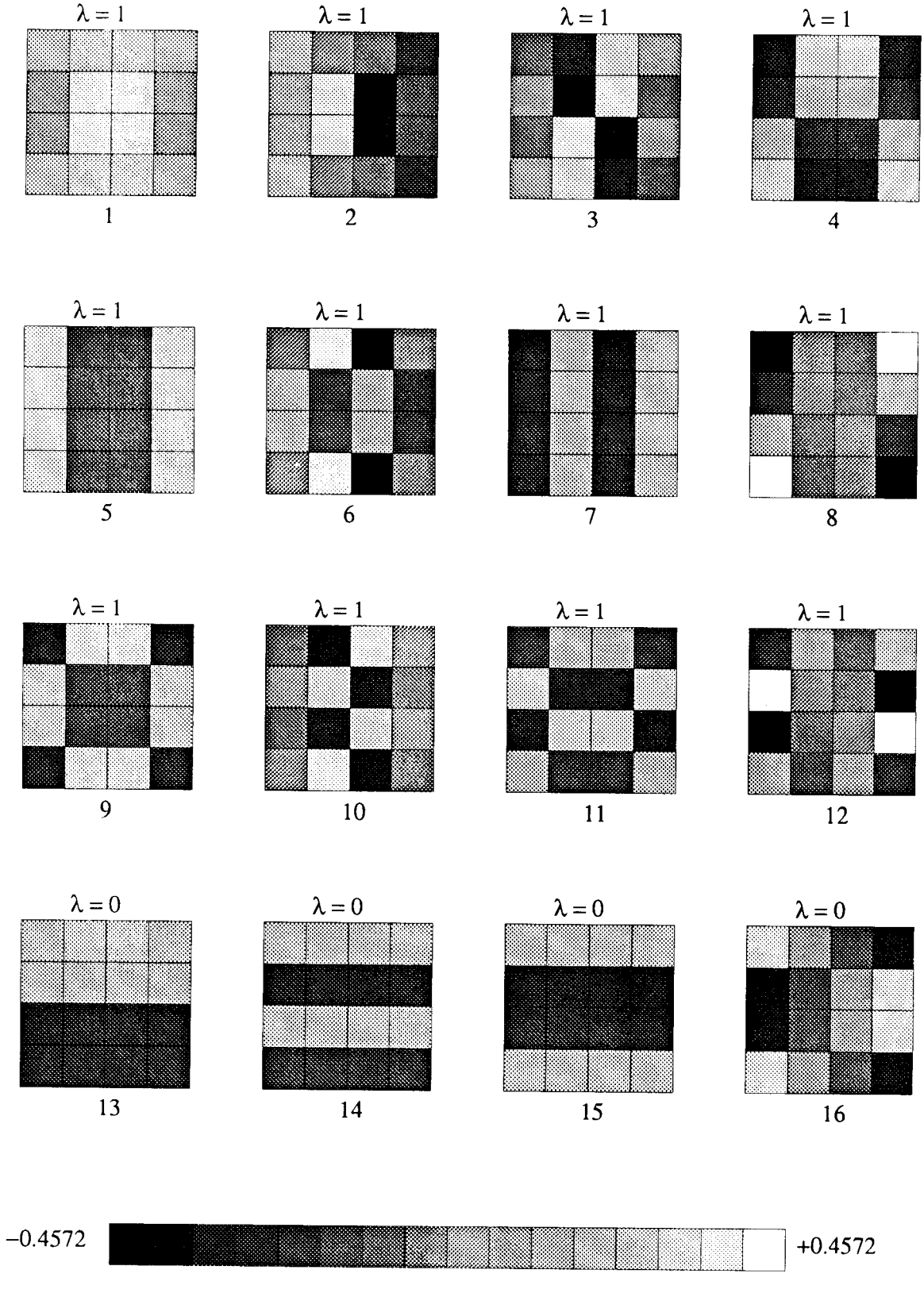

Figure 4. Eigenvectors of the resolution operator associated with the experimental geometry shown in Fig. 1 and with the Lanczos's inversion operator. The first 12 eigenvectors correspond to the degenerate eigenvalue equal to 1. The last four eigenvectors correspond to the degenerate zero eigenvalue. The grey scale is common to the 16 normalized eigenvectors; minimum and maximum values of their components correspond to black and white, respectively.

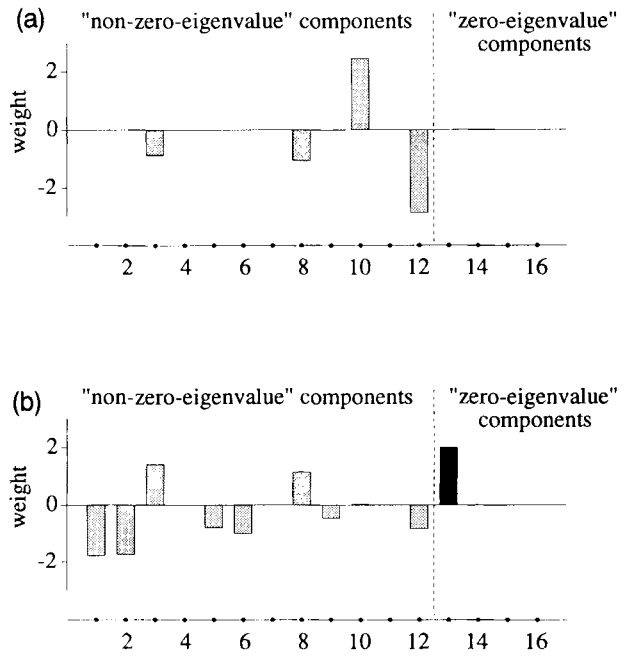

Figure 5. (a) Decomposition of the model shown in Fig. 2(a) on the basis of eigenvectors: The checker-board model has no component in the subspace spanned by eigenvectors related to zero eigenvalues (horizontal axis: index of the eigenvector as numbered in Fig. 4; vertical axis: value of the projection of the model on the corresponding eigenvector of Fig. 4). (b) Decomposition of the model shown in Fig. 3(a) on the basis of eigenvectors; the 'large block' model has a significant component in the subspace spanned by eigenvectors related to zero eigenvalues.

It is interesting to have a look at the resolution operator (Fig. 7) corresponding to our experiment. The diagonal terms are largely dominant and this feature is commonly interpreted as evidence for a high-quality inversion, meaning that the inverted model is close to the actual model. It is clear from the above examples that this intuitive short-cut can be wrong. The reason is that off-diagonal terms viewed as 'small' on the resolution picture, can sometimes build a strong contribution which biases the inverted model. This means that to understand the significance of the resolution operator, one must be aware that the output of a filter depends not only on the characteristics of the filter, but also on its input, as explained in the previous paragraphs.

Another aspect of the problem is the case when some noise is added to the synthetic data before inversion. This new problem can be written as:

$$\mathbf{d}_s = \mathbf{G} \cdot \mathbf{m}_s + \mathbf{n}, \tag{10}$$

leading to:

$$\hat{\mathbf{m}} = \mathbf{R} \cdot \mathbf{m}_s + \mathbf{L} \cdot \mathbf{n}. \tag{11}$$

In this case, the inverted model suffers not only from blurring, as described above but also from contamination due to the propagation of the data noise through the inversion operator. Generally, the inverse operator **L** is designed so that, in addition to other constraints, it minimizes this contamination by keeping the singular values of **L** small, in order to obtain values of $\mathbf{L} \cdot \mathbf{n}$ small as compared with $\mathbf{R} \cdot \mathbf{m}_s$. However, obtaining a final model identical to the initial one is very unlikely when noise is added.

CONCLUSIONS

Inversion of synthetic data can be an appealing way to show how well an inversion scheme works, but, in not uncommon situations, false conclusions may be derived from such experiments. In this note, we have shown by an illustrative example what happens if the model used for the computation of synthetics has the wrong characteristics. We demonstrate that 'wrong characteristics' actually means 'components only in the subspace associated with $\lambda \approx 1$ eigenvalues of the resolution operator'.

In our opinion, the only way to avoid such possible misinterpretations is to make sure that there is a significant component of the model outside this subspace, and in particular in the null space of the resolution operator **R**, which always exists and is never smaller than the null space of the theory operator **G**. The evaluation of this component is always possible in theory. However, this is generally an expensive and sometimes even unfeasible computation, due to the size of the matrix involved.

In our examples, we used the Lanczos's inversion method, but the conclusions are established for any linear inversion method. The only differences follow from the change of non-zero eigenvalues and eigenvectors of **R** when changing the inversion operator **L**. As suggested by a reviewer (W. Menke), it is possible to gain a more significant change in the resolution operator by trying to shrink its null space.

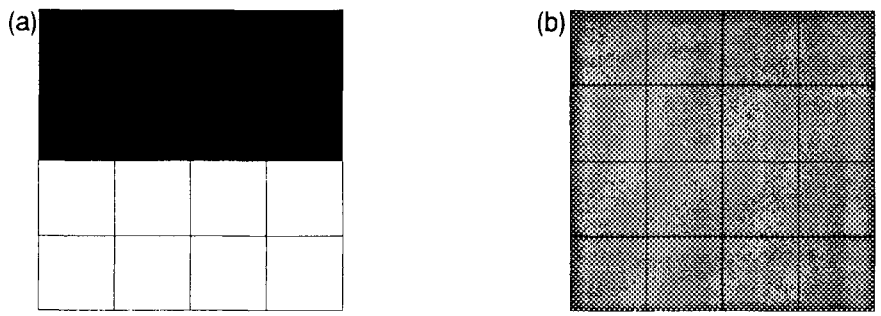

Figure 6. Same as Fig. 2 but for a model which is entirely in the null space of **R** (zero eigenvalues). The inverted model is a flat zero.

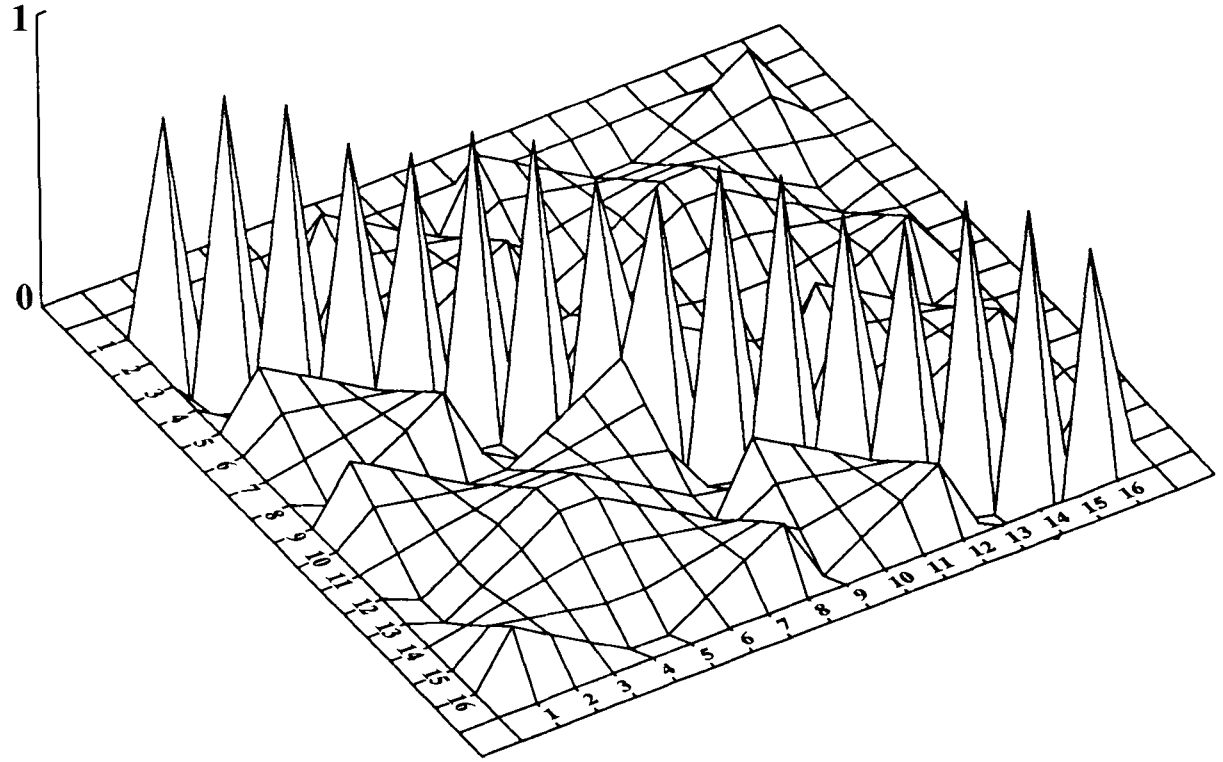

Figure 7. Resolution matrix for the experimental geometry shown in Fig. 1. The elementary blocks of Fig. 1 have been numbered sequentially first from left to right then from top to bottom (block 1 is upper left and block 16 is lower right).

One way to do that is to improve **L** with respect to this, but the ultimate limitation will come from the size of the **G** null space. This limitation can be overcome only by changing **G** itself. In our example, this could be achieved by using a different grid, with a different orientation or a coarser spacing, or by changing the distribution of sources and receivers. A more drastic alternative would be to escape from the linear inversion frame, but this is clearly not within the scope of this note.

The experimental geometry we have chosen to illustrate our point is very simple, but it is representative of a number of real experiments in seismology, such as lithospheric tomography from teleseismic waves and cross-hole tomography, even if real experiments have, generally, a much lower degree of symmetry.

Finally, remember that, in real situations, seismologists know only the second column of Figs 2, 3 and 6 and have to guess the first column, 'which is known only by the gods' (Tarantola 1987, p. 199).

ACKNOWLEDGMENTS

We thank John A. Helm for reading the manuscript and improving its form, and two reviewers, William Menke and Wim Spakman, for helpful comments on the original version of this note. This work has been performed at URA 1358 of CNRS under the INSU grant AA/Tomographie 1992.

REFERENCES

Dziewonski, A. M. & Woodhouse, J. H., 1987. Global images of the Earth's interior, *Science*, **236**, 37–48.

Evans, J. R. & Achauer, U., 1993. Teleseismic velocity tomography using the ACH method: theory and application to continental-scale studies, in *Seismic Tomography: Theory and Practice*, eds Meyer, H. M. & Hirahara, K., Chapman and Hall, London.

Franklin, J. N., 1970. Well-posed stochastic extensions of ill-posed linear problems, *J. Math. Anal. Appl.*, **31**, 682–716.

Fukao, Y., Obayashi, M., Inoue, H. & Nenbai, M., 1992. Subducting slabs stagnant in the mantle transition zone, *J. geophys. Res.*, **97**, 4809–4822.

Lanczos, C., 1961. *Linear Differential Operators*, Chap. 3, Van Nostrand, London.

Montagner, J. P. & Tanimoto, T., 1991. Global upper mantle tomography of seismic velocities and anisotropies, *J. geophys. Res.*, **96**, 20 337–20 351.

Moore, E. H., 1920. Abstract no. 18, *Bull. Am. Math. Soc.*, **26**, 394–395.

Penrose, R., 1955. A generalized inverse for matrices, *Proc. Camb. Phil. Soc.*, **51**, 406–413.

Spakman, W., 1988. Upper mantle delay time tomography with an application to the collision zone of the Eurasian, African and Arabian plates, *Dissertation*, No. 53, Rijksuniversitet Utrecht.

Tarantola, A., 1987. *Inverse Problem Theory*, Elsevier Science Publishers, Amsterdam.

Trampert, J. & Lévêque, J.-J., 1990. Simultaneous Iterative Reconstruction Technique: physical interpretation based on the Generalized Least Squares solution, *J. geophys. Res.*, **95**, 12 553–12 559.